Environmental Research Letters

LETTER

Identification of deficiencies in seasonal rainfall simulated by CMIP5 climate models

Caroline M Dunning[1,4], Richard P Allan[1,2,3] and Emily Black[1,2]

[1] Department of Meteorology, University of Reading, Reading, United Kingdom
[2] NCAS-Climate, University of Reading, Reading, United Kingdom
[3] National Centre for Earth Observation (NCEO), University of Reading, Reading, United Kingdom
[4] Author to whom any correspondence should be addressed.

E-mail: c.m.dunning@pgr.reading.ac.uk

OPEN ACCESS

RECEIVED
23 March 2017

REVISED
11 August 2017

ACCEPTED FOR PUBLICATION
16 August 2017

PUBLISHED
26 October 2017

Keywords: Africa, precipitation, seasonality, CMIP5, Little Dry Season (LDS), model evaluation, AMIP

Supplementary material for this article is available online

Abstract

An objective technique for analysing seasonality, in terms of regime, progression and timing of the wet seasons, is applied in the evaluation of CMIP5 simulations across continental Africa. Atmosphere-only and coupled integrations capture the gross observed patterns of seasonal progression and give mean onset/cessation dates within 18 days of the observational dates for 11 of the 13 regions considered. Accurate representation of seasonality over central-southern Africa and West Africa (excluding the southern coastline) adds credence for future projected changes in seasonality here. However, coupled simulations exhibit timing biases over the Horn of Africa, with the long rains 20 days late on average. Although both sets of simulations detect biannual rainfall seasonal cycles for East and Central Africa, coupled simulations fail to capture the biannual regime over the southern West African coastline. This is linked with errors in the Gulf of Guinea sea surface temperature (SST) and deficient representation of the SST/rainfall relationship.

1. Introduction

The timing and seasonality of precipitation is of critical importance to the many African stakeholders who depend upon the seasonal rains for agricultural and domestic purposes. Failure or delays in these rains can lead to significant socio-economic impacts (Vizy *et al* 2015). Future changes in climate will be felt not only through changes in mean precipitation, but also through altered seasonality, which in turn influences the growing season and crop yields (Vizy *et al* 2015), the length of the malaria transmission season (Tanser *et al* 2003), the supply of hydroelectric power (Yamba *et al* 2011, van Vilet *et al* 2016) and surface water supplies (de Wit and Stankiewicz 2006). Producing reliable projections of the impact of climate change in a range of sectors therefore requires an accurate representation of seasonality within the climate projections being utilized.

Seasonality is sensitive to changes in atmospheric circulation patterns (Shongwe *et al* 2009, Lee and Wang 2014) and diagnosing and interpreting such changes requires a robust understanding of the dynamics and drivers of the seasonal cycle. In order to use global climate models (GCMs) to investigate the physical mechanisms driving the seasonal cycle of precipitation, and assess the reliability of future impact projections, it is necessary that GCMs are able to represent the seasonality of African precipitation.

In this study we take a continental scale approach to the assessment of the seasonality of African precipitation in the Atmospheric Model Intercomparison Project (AMIP) and historical experiments as part of the Coupled Model Intercomparison Project Phase 5 (CMIP5) simulations (Taylor *et al* 2012). An objective technique is applied using cumulative rainfall anomaly to calculate the onset and cessation of wet seasons (Liebmann *et al* 2012, Dunning *et al* 2016). This technique enables examination of the nature of the seasonal cycle, in terms of the number of wet seasons experienced per year (seasonal regime), the patterns of rainfall advance and retreat, and the timing of the wet seasons.

This paper aims to address three main questions:

- Can models realistically represent contrasting annual and biannual seasonal precipitation regimes across the continent?
- How well is the seasonal progression of rainfall represented, including spatial patterns of rainfall advance and retreat throughout the year?
- How well is the timing of the rainy seasons captured?

Many previous studies examining the representation of African precipitation in CMIP models have assessed mean rainfall amount and interannual variability for fixed seasons (Kumar *et al* 2014, Lee and Wang 2014, Mehran *et al* 2014, Maidment *et al* 2015). Those studies that do consider the seasonal cycle of precipitation either take averages over large areas, smoothing out much of the variability, and neglecting the seasonal progression of the rains (Dike *et al* 2015) or use metrics such as seasonality skill score (Koutroulis *et al* 2016), sum of squared errors (Yamana *et al* 2016), or space-time root-mean-square error (Flato *et al* 2013) which primarily focus on long-term monthly data. The methodological approach used here enables comparison between models, notwithstanding timing discrepancies. Additionally, the proven agricultural relevance of this onset/cessation metric means this evaluation of climate models is informative for impact studies (Dunning *et al* 2016).

Studies that examine the onset and cessation of rainfall in climate models, taking into account the seasonal progression of rains, have previously focused on specific regions such as East Africa (McHugh 2005, Yang *et al* 2015a), Southern Africa (Dedekind *et al* 2016) and the Sahara (Liu *et al* 2002). The continental approach taken here complements these regional studies, providing insight into the links between timing biases in different regions and the links with large-scale progression of the wet season across regions. Several of the previous studies into seasonality have used regional climate models, such as the CORDEX regional models (West Africa: Mounkaila *et al* 2015, Southern Africa: Shongwe *et al* 2015, East Africa: Endris *et al* 2013). While these models are valuable in providing regional detail, they are driven at their lateral boundaries by GCMs, and therefore understanding the seasonality in GCMs remains of key importance. Furthermore, some impact projections use GCMs, and few conduct thorough assessments of the representation of precipitation seasonality, potentially using models with significant deficiencies in seasonality representation (Yamba *et al* 2011, Hamududu and Killingtveit 2012, Caminade *et al* 2014, van Vilet *et al* 2016). The United Nations Development Programme (UNDP) Climate Change Country Profiles contain multi-model mean projections of annual and seasonal temperature and precipitation for a range of developing countries and were designed to facilitate climate change assessment with minimal computational expense (McSweeney *et al* 2010), and are currently utilised in both agricultural (Adhikari *et al* 2015) and ecological (Laloë *et al* 2014) sectors. However, the same set of 15 GCMs are used for all countries, and hence multi-model mean projections in the locally-defined seasonal means may be inaccurate if the models used contain seasonal cycle timing biases.

This study presents, for the first time, a continent-wide evaluation of climate model representation of African rainfall seasonality. It aims to better characterise the representation of the seasonal cycle in terms of regime, progression and timing, in order to provide more detail on model deficiencies and their causes, and to facilitate better application of such models for climate change impact assessments.

2. Methods and data

In order to assess rainfall seasonality in terms of seasonal regime (annual or biannual), progression and timing, we apply the method of Dunning *et al* (2016) which extends the methodology of Liebmann *et al* (2012). Firstly, at each grid point the ratio between the amplitude of the first and second harmonics is computed to determine whether an annual (one wet season/year) or biannual (two wet seasons/year) regime dominates. Secondly, the period of the year when the wet season occurs is determined by identifying the minima and maxima in the climatological cumulative daily mean rainfall anomaly, to account for seasons that span multiple calendar years. Dunning *et al* (2016) introduces a method for doing this for biannual regimes, accompanying the method for annual regimes in Liebmann *et al* (2012). Following the identification of the climatological seasons, onset and cessation dates are calculated for each season and year individually by identifying the minima and maxima in the daily cumulative rainfall anomaly over that season. The climatological cumulative daily mean rainfall anomaly and daily cumulative rainfall anomaly are computed independently for each climate model and dataset. Onset and cessation dates are not calculated for the first or last years of each dataset. The approach was found to be applicable for datasets with contrasting rainfall biases, producing contemporaneous onset/cessation dates (Dunning *et al* 2016), and thus can be applied to model simulations without the need for bias correction. The method also permits seasons to span different time periods thus enabling the examination of timing differences and comparison of wet seasons that do not coincide exactly across models and observations. By comparison with agricultural onset methods proposed by Marteau *et al* (2009), Issa Lélé and Lamb (2010), and Yamada *et al* (2013), Dunning *et al* (2016) demonstrate the relevance of this method to agricultural stakeholders.

For calculation of onset and cessation dates, daily precipitation data is required. Forty-six models

were chosen from the CMIP5 generation of models (Taylor *et al* 2012), based on the availability of daily precipitation for an AMIP simulation (which applies observed sea surface temperature (SST) and sea ice and realistic radiative forcings) or CMIP5 historical simulation (which includes a fully coupled ocean and is driven by historical radiative forcings) from the British Atmospheric Data Centre (BADC). 28 AMIP simulations were used over 1979–2008 and 39 CMIP historical simulations were used over 1979–2005 (some variations in dates; supplementary table S1, available at stacks.iop.org/ERL/12/114001/mmedia). Models, name of institute and horizontal resolution are listed in table S1. Only the first ensemble members (r1i1p1) are considered since differences across ensemble members were found to be minimal, and much smaller than the inter-model differences.

To allow construction of multi-model means, the data were re-gridded using bilinear interpolation to the GPCP 1DD 1° × 1° grid. For some models this is a large increase in resolution; results were compared using a 2° × 2° grid for the CMIP historical simulations and found to be unchanged. Following re-gridding, onset and cessation dates were calculated. For the individual model results in the supplementary information, the method is applied at native resolution (table S1).

In order to compare rainfall over the southern West African coastline and SSTs over the Gulf of Guinea (section 4), monthly SST data was obtained for 37 of the 39 historical simulations from BADC. Monthly HadISST observed SST and monthly AMIP forcing SST data were obtained at 1° × 1° horizontal resolution.

A reference dataset was required for comparison, to facilitate the assessment of the ability of CMIP5 model simulations to represent seasonality over Africa. Inaccuracies in ERA-Interim reanalysis precipitation data have been identified (Hill *et al* 2016, Dunning *et al* 2016) and thus reanalysis data was not used. To account for uncertainties in some datasets (Maidment *et al* 2014) five different satellite based precipitation datasets available at daily resolution were exploited (table S2): the African Rainfall Climatology version 2 (ARCv2) precipitation dataset (Novella and Thiaw, 2013), the Climate Hazards Group InfraRed Precipitation with Stations (CHIRPS) dataset (Funk *et al* 2015), the Global Precipitation Climatology Project 1 Degree Daily (GPCP 1DD) product (Huffman *et al* 2001), the TAMSAT (Tropical Applications of Meteorology using SATellite data and ground-based observations) African Rainfall Climatology and Timeseries (TARCATv2) dataset (Maidment *et al* 2014, Tarnavsky *et al* 2014, Maidment *et al* 2017) and the Tropical Rainfall Measuring Mission (TRMM) Multisatellite Precipitation Analysis (TMPA) 3B42 research derived daily product (Huffman *et al* 2007). Temporal coverage and horizontal resolution are shown in table S2. They were all re-gridded to the 1° × 1° GPCP 1DD grid for all analysis (including supplementary information).

For analysis of timing, Africa was divided into a number of regions (figure S1). These were chosen to primarily exhibit an annual or biannual regime and contain broadly similar onset and cessation dates. The area north of 15°N was not included in the analysis due to the dry climate. The GPCP annual/biannual categorisation was used as a basis for the region mask; model simulation grid-points were considered as belonging to a region if they fell within the correct geographical area and had the correct annual/biannual categorisation. Hence figure S1 shows the maximum possible extent of the regions; for some models fewer points were included if they had an incorrect categorisation.

Figure 1 illustrates the application of the Dunning *et al* (2016) method over the Horn of Africa and the Sahel (region map: figure S1/4(*b*)). Average rainfall rate in each of the four/two seasons is calculated for the long term climatology (all available years; coupled: 1980–2004, atmosphere-only: 1980–2007, observations: 1982–2013) for standard meteorological seasons (Horn of Africa: short rains October–December, long rains March–May; Sahel: wet season July–September, dry season October–June; hashed bars) and when the seasons are determined dynamically for each model and year (solid bars) using the method of Dunning *et al* (2016) which allows seasons to shift in space and time from year to year and across different models. Rainy seasons are differentiated more clearly from the dry seasons when the seasons are determined dynamically, as the method accounts for interannual variability in seasonal timing and model timing biases. This better seasonal distinction is obtained for all regions (figures S2–S3) with wet/dry season difference in average rainfall rate 33% larger when seasons are defined dynamically (annual regions). This demonstrates the advantage of examining seasonality using a method that objectively identifies wet seasons in models, and would enable the analysis of future changes in seasonality, while accounting for errors in the mean state. The socio-economic importance of the East African long rains, necessitates extensive climate model analysis of this season, where use of a method that better distinguishes the long rains (as seen in figure 1(*a*)) would facilitate more meaningful model analysis and inter-model comparison (Lyon and DeWitt 2012, Tierney *et al* 2015). Due to prior assessment (Flato *et al* 2013, Kumar *et al* 2014, Koutroulis *et al* 2016) the magnitude of the seasonal cycle is not explicitly examined here, however, similar average rainfall rates (figures 1 and S2–3) indicates agreement in seasonal cycle amplitude across observations, atmosphere-only, and coupled simulations for all regions.

3. Results

First the representation of annual and biannual seasonal regimes in the model simulations is examined.

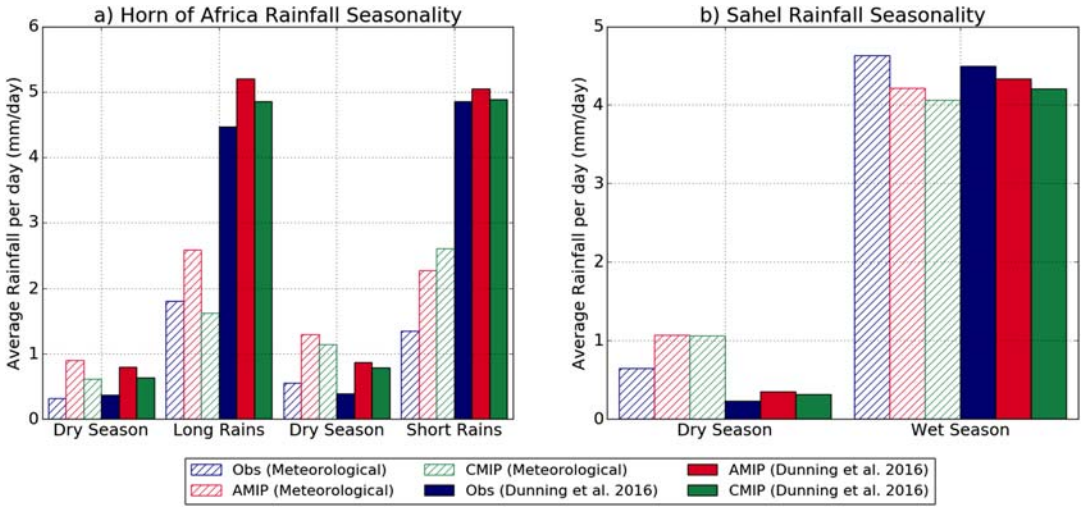

Figure 1. Average rainfall rate (mm day^{-1}) during the wet/dry seasons over the Horn of Africa (*a*) and the Sahel (*b*) when defined using meteorological seasons (dashed bars) and dynamically varying seasons (Dunning *et al* 2016, solid). The same set of simulations was used for both meteorological and dynamically varying seasons. See figure S1 for a map of the regions.

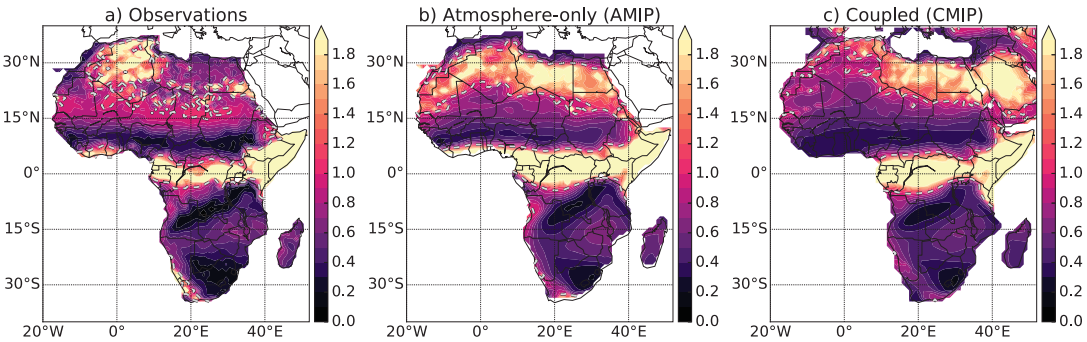

Figure 2. The mean ratio of the amplitude of the harmonic at two cycles/year to the amplitude of the harmonic at one cycle/year for (*a*) observations, (*b*) atmosphere-only (AMIP) and (*c*) coupled (CMIP historical) simulations. The dotted line shows where the ratio is equal to 1.0.

The multi-model mean ratio of the second harmonic to first harmonic for observations, atmosphere-only simulations and coupled simulations are shown in figures 2(*a*)–(*c*) (individual model plots; figures S4-S7). A ratio greater than 1.0 indicates a biannual regime, whereas a ratio of less than 1.0 indicates an annual regime.

In Africa the biannual regime covers three zones: the Horn of Africa (Camberlin *et al* 2009, Yang *et al* 2015b), a zonal equatorial strip from Equatorial Guinea to Uganda (Diem *et al* 2014) and a small region on the south West Africa coastline (hereafter referred to as SWAC) (Sultan and Janicot 2003, Herrmann and Mohr 2011) (figure 2(*a*)). The atmosphere-only simulations capture the biannual regime over these regions (figure 2(*b*)), and while the area experiencing a biannual regime is larger than in the observations, there is good agreement between figures 2(*a*) and (*b*). While the coupled simulations capture the biannual regime for the Horn of Africa and the equatorial strip, the biannual regime over SWAC is not represented (figure 2(*c*)). The lack of such a season over Nigeria in HadGEM2-ES has also been identified by Dike *et al* (2015), but causes were not attributed. In both experiments an annual regime is found over southern Africa, West Africa and the Sahel, as in the observations.

Secondly, the representation of the spatial patterns of seasonal progression of precipitation is examined. Figure 3 shows the multi-model mean onset and cessation dates for both annual and biannual regimes. The patterns in observations (figures 3(*a*),(*d*),(*g*) and (*j*)) are in agreement with those in Liebmann *et al* (2012) and Dunning *et al* (2016). The broadly meridional progression of onset and cessation dates across West Africa and the Sahel is represented by both multi-model means, with northward progression of onset in the boreal spring following on smoothly from the onset of the first/long rains (figures 3(*a*)–(*c*)), and southward progression of cessation in the boreal autumn preceding the end of the second/short rains (figures 3(*d*)–(*f*)). The later onset over northwest Senegal and surrounding areas in comparison with other points of the same latitude (Marteau *et al* 2009) is also apparent

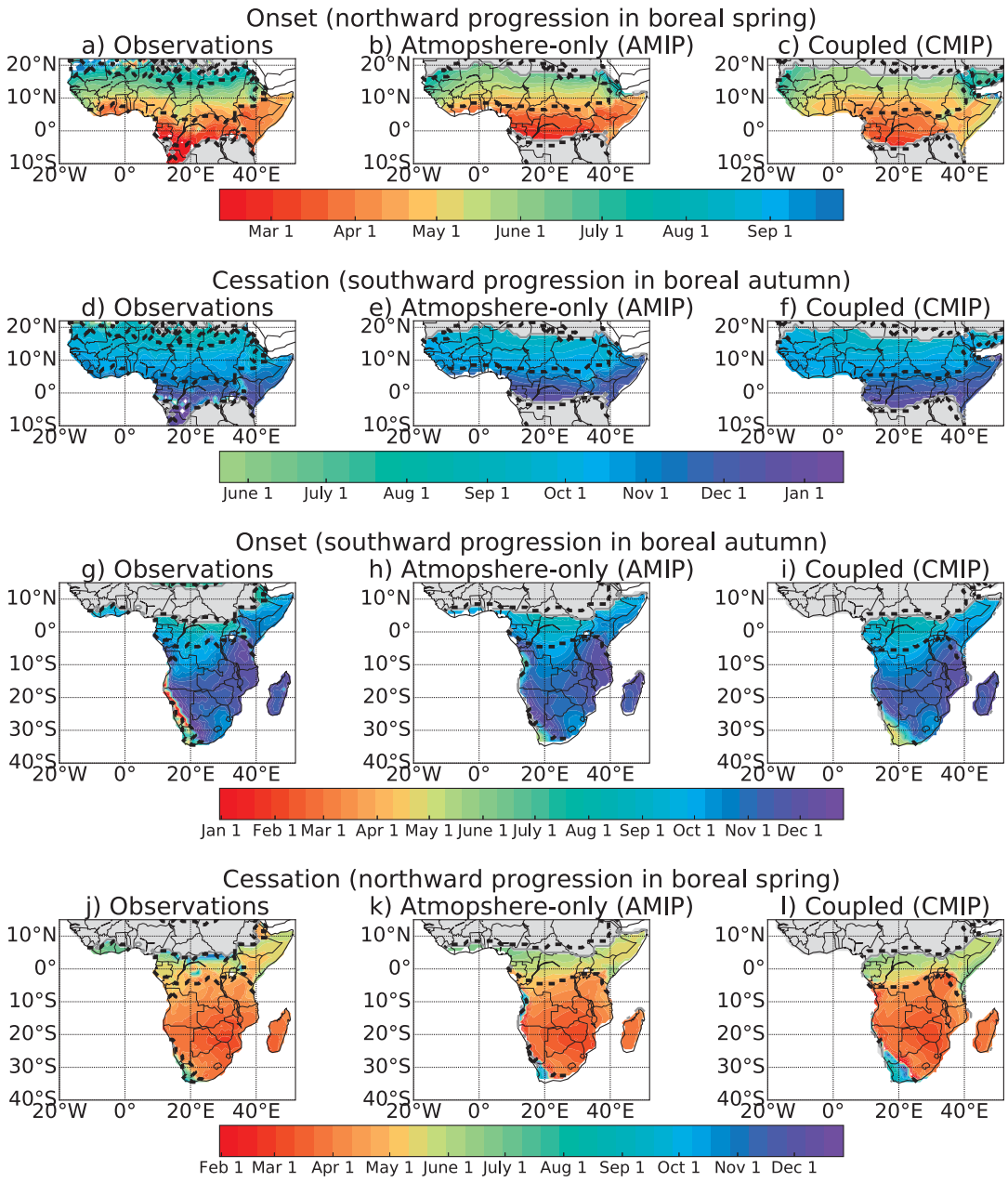

Figure 3. Seasonal progression of onset/cessation of wet seasons in observations (*a*), (*d*), (*g*) and (*j*), atmosphere-only (AMIP) (*b*), (*e*), (*h*) and (*k*) and coupled (CMIP) simulations (*c*), (*f*), (*i*) and (*l*). Onset/cessation in annual regime regions is plotted with onset/cessation in biannual regions to demonstrate continuous progression across annual/biannual boundaries (denoted by dashed black lines). (*a*)–(*c*) Northward progression of onset in boreal spring from first/long rains into West African Monsoon (WAM). (*d*)–(*f*) Southward progression of cessation in boreal autumn from the WAM into end of second/short rains. (*g*)–(*i*) Southward progression of onset in boreal autumn, from second/short rains into the annual rains over southern Africa. (*j*)–(*l*) Northward progression of cessation in boreal spring from the end of the annual rains over southern Africa into first/long rains. Grey indicates regions not considered for these plots.

in figures 3(*a*)–(*c*). Christensen *et al* (2013) found models fail to capture central features of the West African Monsoon, yet we find realistic representation of the seasonal progression over West Africa. Over central and southern Africa, onset commences in the north-west and south-east, following the onset of the second/short rains; a pattern seen in observations, and both multi-model means. Figures 3(*j*)–(*l*) all exhibit the radial spreading of cessation, commencing on the Mozambique/Zimbabwe/South Africa border, leading into the cessation of the first/long rains. The main difference is found over the south west tip of South Africa; the winter rainfall regime experienced here (as opposed to the summer regime experienced in the majority of the country) (Weldon and Reason 2014, Engelbrecht *et al* 2015) covers a larger area in the coupled simulations (figures 3(*i*) and (*l*)) than in atmosphere-only simulations and observations (figures 3(*g*), (*h*), (*j*) and (*k*)). Dedekind *et al* (2016) also found discrepancies over southern Africa where the summer rainfall peak was two months early in CCAM (AMIP). Correspondingly, individual models (figures S8–23) demonstrate seasonal progression in agreement with that found in the observations.

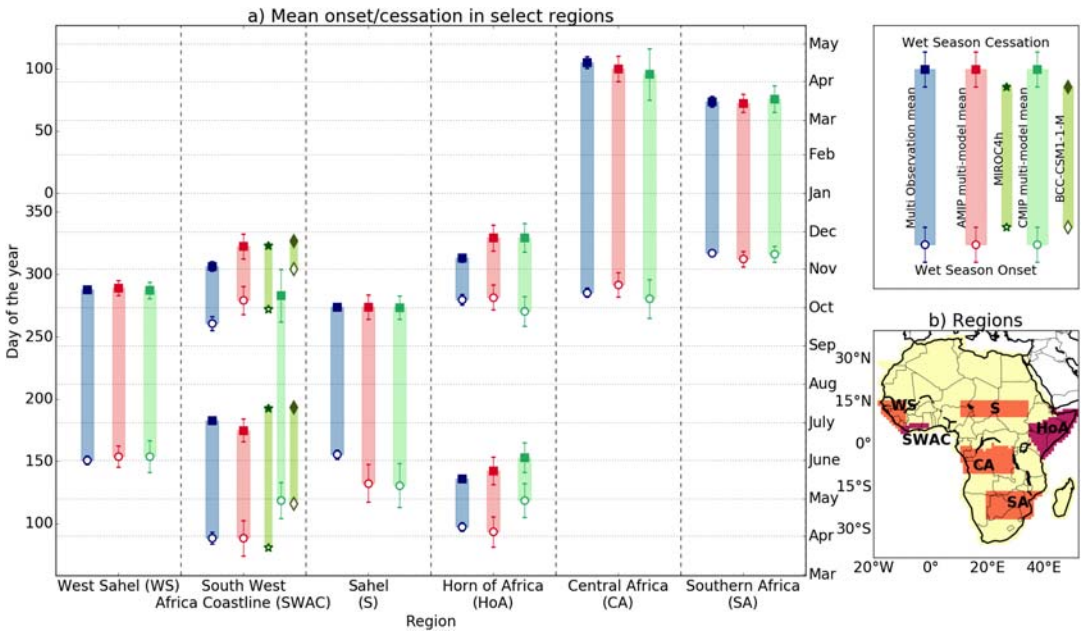

Figure 4. Mean onset (open circles) and cessation (filled squares) for selected regions (see (*b*)). Multi-model mean for observations, atmosphere-only (AMIP) and coupled (CMIP) simulations are plotted with the errorbars indicating standard deviation over individual model means for each region. Shaded bars indicate the period of the wet season. For SWAC the mean annual regime onset/cessation in coupled simulations is plotted, along with mean onset/cessation for MIROC4h and BCC-CSM1-1-M (coupled simulations), the only coupled simulations to capture a biannual regime here.

The third aspect of seasonality examined was seasonal timing (figure 4), full results for all models and regions (figure S1) are in figures S24–S26. The multi-model mean onset and cessation dates for five of the regions (figure 4(*a*)) show the models generally simulate the wet season at the correct time of year. Notable differences include early onset over the Sahel (23 ± 15 days on average for atmosphere-only, 25 ± 18 days for coupled simulations, where the error relates to standard deviation across models), longer short rains over the Horn of Africa (cessation ∼16 ± 11 days later) and later long rains (onset/cessation ∼19 ± 13 days late for coupled simulations) over the same region. The late bias of the long rains in coupled simulations, with cessation in early June (on average) may explain some of the dry bias previously found in the long rains over East Africa in CMIP5 models (Yang *et al* 2015a). The overestimation of the short rains, typically found in such models (Yang *et al* 2015a), is replicated here in the combination of longer season length, of 14 ± 14 days longer for AMIP and 25 ± 15 days longer for CMIP historical simulations (figure 4(*a*)), and similar average rainfall per day (figure 1(*a*)).

Most coupled simulations do not capture the biannual regime over SWAC (figure 2(*c*)), hence the mean onset and cessation dates for the annual regime over this region are shown in figure 4(*a*), while the season over SWAC is longer than is found over the west Sahel, it is shorter than atmosphere-only and observations for SWAC, with onset occurring during the first rains, and cessation occurring during the second rains. Biannual onset and cessation dates for one of the two coupled simulations that simulate a biannual regime here (MIROC4h and BCC-CSM1-1-M) show good agreement with observations, but the onset dates are late in BCC-CSM1-1-M.

Mean onset and cessation dates were computed for each simulation for 13 regions with an annual regime (see figure S1) and the Horn of Africa, and compared with mean observational onset and cessation dates. For atmosphere-only simulations the mean difference from observations for onset ranged between −18 ± 14 days to +6 ± 10 days (negative values denote early onset, positive is late), with the onset over the Sahel exhibiting larger differences of −23 ± 15 days. Cessation dates exhibited smaller mean differences, with differences ranging between −5 ± 10 days to 8 ± 15 days for the different regions. For coupled simulations the mean difference from observations for onset ranged from −15 ± 10 days to +3 ± 13 days, with larger differences over the Sahel (−25 ± 18 days) and over the west coast of southern Africa. The discrepancy over this southern region is likely to be related to overestimation of the area that experiences a winter rainfall regime shown in figure 3, and exclusion of dry areas associated with the Namibian Desert (Liebmann *et al* 2012, Engelbrecht *et al* 2015). For cessation, differences from the observations are of similar magnitude, with differences ranging from −12 ± 10 days to +15 ± 11 days, with the west coast of southern Africa again an outlier, showing a much higher value. Individual results for each model and region are included in the supplementary information.

Overall, figures 2–4 (and figures S4–S23) indicate that the model simulations realistically capture the seasonal progression of the rainy seasons over Africa.

However, coupled simulations overestimate the areal extent of the winter rainfall regime in South Africa, leading to large timing errors over South Africa (40–50 days on average, region 15 in figures S24–S25) and importantly fail to capture the biannual regime over SWAC. The potential for detrimental impacts of the intervening dry season on agricultural yields (Odekunle, 2007) coupled with high population density (Global Urban-Rural Mapping Project (GRUMP) 2000), and changing nature of the seasonality (Chineke *et al* 2010), motivated further exploration of this misrepresentation (section 4).

4. Simulation of the Little Dry Season in southern coastal West Africa

The biannual regime over SWAC comprises four seasons; a dry season from November–March, the first wet season from April–June and the second wet season from mid–September–October. These two wet seasons are separated by a break in the monsoon rains during July–August, known as the 'August Break' (Chineke *et al* 2010) or 'Little Dry Season' (LDS) (Odekunle 2010). The LDS can be a useful period for weeding and spraying of crops; when the LDS is too early, long or intense, yields can be reduced (Adejuwon and Odekunle, 2006). Both the mean annual cycle of precipitation in observations (blue line) and atmosphere-only (red line), over the LDS region (figure 5(*b*)), show the biannual seasonal cycle. However, figure 5(*b*) confirms that coupled simulations (green line) do not capture the correct seasonal cycle.

The misrepresentation of the Little Dry Season is related to the southward Intertropical Convergence Zone (ITCZ) bias in coupled simulations (Richter and Xie 2008, Roehrig *et al* 2013, Toniazzo and Woolnough 2014, Monerie *et al* 2017). This bias has been connected with the presence of warm Atlantic SST biases in the Gulf of Guinea (Vizy and Cook 2001, Cook and Vizy 2006, Roehrig *et al* 2013), via influences on the meridional temperature gradient. Furthermore, the strength of the West African Monsoon is sensitive to SSTs in the equatorial cold tongue (Patricola *et al* 2012), such that sporadic warming in this region resulting from Atlantic Niños (Nnamchi *et al* 2015) weakens the monsoon circulation and monsoon rains are confined to the Guinea Coast (Chang *et al* 2008). Hence, the failure of the coupled simulations to reproduce the eastern equatorial cold tongue in boreal summer (Richter and Xie 2008, Patricola *et al* 2012) may be associated with the restricted northward progression of the ITCZ. More locally, the reduction in rainfall during the LDS is accompanied by cool SSTs in the northern Gulf of Guinea, in particular, between 8°W–2°E, and 3°N to the West African coastline (figure 5(*a*), pink box), resulting from ocean upwelling (Odekunle and Eludoyin 2008) (figure 5). Adejuwon and Odekunle (2006) proposed that the LDS was a consequence of these local cooler SSTs leading to the inter-tropical discontinuity travelling further inland, while Odekunle and Eludoyin (2008) suggested that cool SSTs increased static stability over this region, inhibiting convection.

The correct representation of the LDS in atmosphere-only simulations with prescribed SSTs and incorrect representation in fully coupled simulations (figure 5(*b*)), combined with previous research (Adejuwon and Odekunle 2006, Odekunle and Eludoyin 2008), suggests an SST driver for the LDS. Thus the relationship between SSTs in the northern Gulf of Guinea region (8°W–2°E, and 3°N to the West African coastline; pink box in figure 5(*a*)), and LDS rainfall is explored to determine if this could explain the misrepresentation (figure 5). Observational datasets were used to determine the mean period of the LDS (2 July–17 September), and the region influenced by this regime (SWAC; blue dots in figure 5(*a*)). Linear regression was used to examine the relationship between LDS rainfall and July–August–September (JAS) SST (figure 5(*c*)). Observations and atmosphere-only simulations exhibit the expected relationship with colder SST anomaly years resulting in lower LDS rainfall, yet coupled simulations fail to represent this association (figure 5(*c*)). In addition, none of the coupled simulations realistically represent the SST seasonal cycle over the region of interest identified by Adejuwon and Odekunle (2006), the minima are in September rather than August, and the amplitude of the SST seasonal cycle is only ~55% of that in HadISST, at 2.3 K compared with 4.3 K in HadISST and 4.1 K in AMIP.

The coupled historical simulations for MIROC4h and BCC-CSM1-1-M contain an LDS at a few coastal grid-points, evident in most ensemble members, and also exhibit SST anomalies in the lowest 10% for July and August, compared with all coupled simulations (brown/pale pink dashed line, figure 5(*d*)).

These findings are consistent with the lack of a LDS in coupled simulations being related to unrealistic representation of the SST seasonal cycle, and an incorrect interannual relationship between SST and rainfall. The seasonal cycle of SST is an important driver of seasonality in rainfall, with previous studies identifying a significant influence of the decline in equatorial SST from April to July on the development of the monsoon (Okumura and Xie 2004) and a delay in the phase of the Atlantic SST seasonal cycle resulting in an increase in late rainy season precipitation (Monerie *et al* 2017). It may be inferred therefore that models that represent SST seasonality well are more likely than others to capture the seasonality of rainfall accurately. However, a good representation of SST is not the only factor in determining models' ability to capture rainfall. When analyzing the Atlantic ITCZ structure, Siongco *et al* (2015) found that model horizontal resolution had a large influence on the marine ITCZ. MIROC4h and BCC-CSM1-1-M have higher spatial resolution than many of the other models used

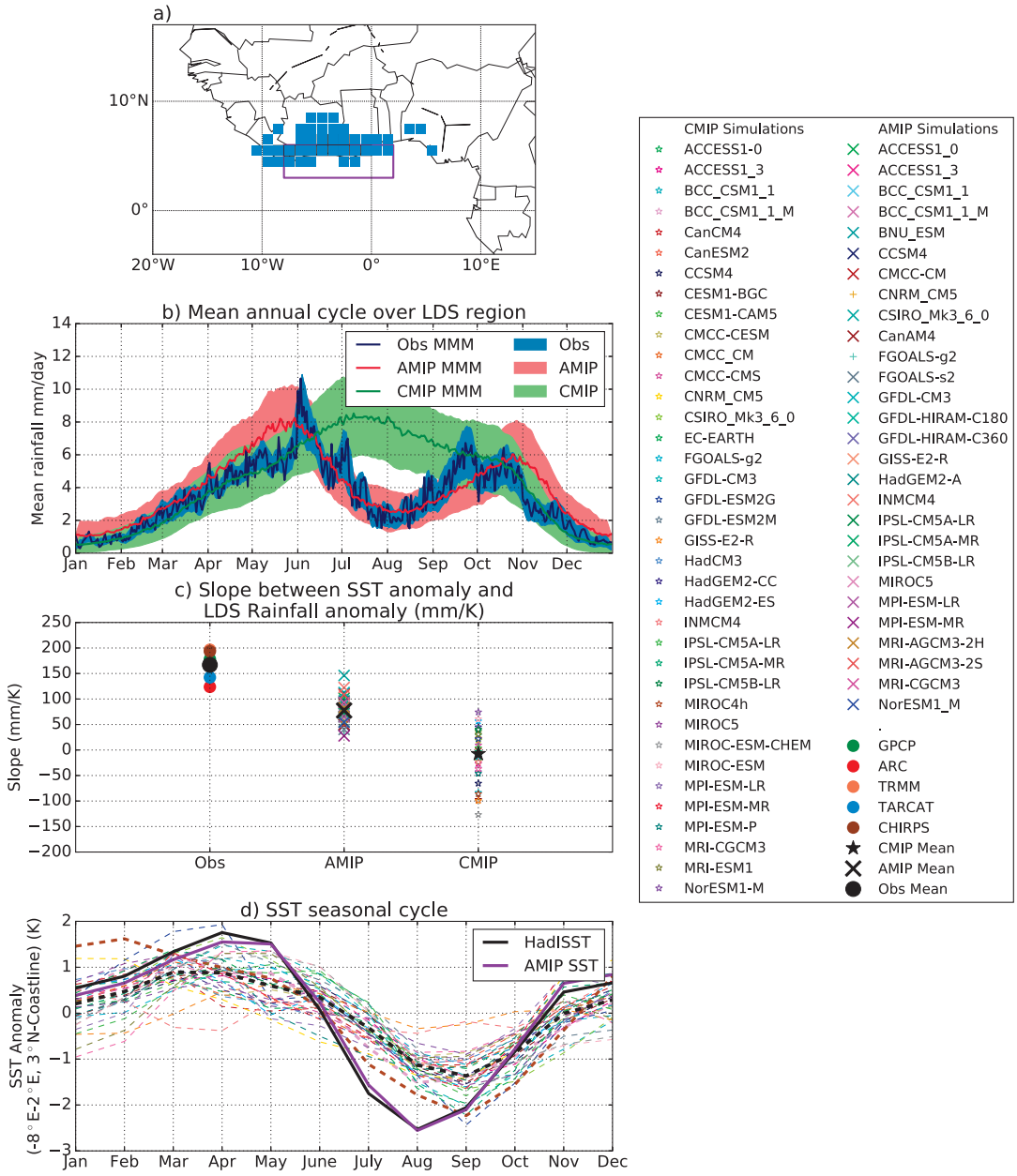

Figure 5. Rainfall and SST links over SWAC and neighbouring ocean. (*a*) Location of the region that experiences the Little Dry Season (LDS; blue dots) and the SST region of interest (pink box). (*b*) Mean annual cycle of rainfall in observations, atmosphere-only and coupled simulations over the LDS region (blue dots in (*a*)). (*c*) Slope of the linear regression between interannual variations in LDS rainfall (rainfall during 2 July–17 September) and July–August–September SST. Filled symbols indicate statistical significance of the slope at the 95% significance level (crosses for AMIP). (*d*) Seasonal cycle of SST in HadISST, AMIP and coupled simulations, with the black dotted line indicating the coupled multi-model mean.

and better representation of the SST seasonal cycle, with lower SST anomalies in JAS. Yet, it would be over-simplistic to argue that resolution and accurate representation of SST alone determine models' ability to capture the LDS at a few grid points. Monerie *et al* (2017) noted that the influence of SST varies across climate models, which may explain why some models with similar SST seasonal cycle and resolution (e.g. EC-Earth) do not contain an LDS. Of the 18 models analysed by Cook and Vizy (2006) only four correctly captured the relationship between Gulf of Guinea SST anomalies and West African Monsoon precipitation anomalies; hence even with the correct SST the coupled simulations may not produce a LDS due to inaccurate representation of the variability. Furthermore, the monsoon acts to cool SST (Okumura and Xie 2004, Hagos and Cook 2009), hence correct representation of SST seasonality is both a cause of and response to the accuracy of precipitation seasonality. The preceding discussion thus highlights two likely causes of model bias in the representation of the West African Monsoon and provokes a number of additional questions. Further detailed analysis of such mechanisms is merited, along with other LDS drivers, including the deflection of south-westerly winds to westerly winds (Olaniran 1989), which could be addressed through

idealized model integrations and further analysis of observations.

5. Conclusions

The representation of precipitation seasonality in atmosphere-only and coupled historical CMIP5 climate model simulations has been evaluated across Africa using observations and an objective methodology for quantifying seasonal characteristics (Liebmann *et al* 2012, Dunning *et al* 2016). Using this methodological approach demonstrates the presence of a biannual regime over regions with timing biases, where the use of standard meteorological seasons may suppress the perceived seasonal cycle, and thus can be used to compare model simulations, notwithstanding timing biases.

Overall, the CMIP5 simulations capture the gross seasonal cycle of African precipitation on a continental scale. The patterns of seasonal progression of the rainy season are well-represented, and the atmosphere-only simulations realistically simulate biannual rainfall regimes for the Horn of Africa, Equatorial Africa and a region on the southern West Africa coastline (SWAC). Patterns of seasonal progression over southern Africa are the consequence of interactions between the ITCZ, the South Atlantic Anticyclone, mid latitude westerlies and the Angola Low, where the tropical–extratropical cloud bands that bring summer rainfall across southern Africa form (Reason *et al* 2006). The large-scale similarity in spatial rainfall progression patterns over Southern Africa across observations, atmosphere-only and coupled integrations suggest that the models capture these interactions which lead to the non-zonal patterns observed in this region (Reason *et al* 2006, Shongwe *et al* 2009, Shongwe *et al* 2015). Seasonal timing in atmosphere-only simulations demonstrates good agreement with observations (most mean onset/cessation dates agree within 18 days) although both sets of simulations exhibit an early onset of the wet season over the Sahel (~25 days early). Additionally, coupled simulations exhibit timing biases over the Horn of Africa (long rains ~20 days late).

Although the seasonal cycle is generally represented well in atmosphere-only model runs, in regions influenced by annually changing SST, SST biases in coupled simulations lead to errors in rainfall patterns. The incorrect annual seasonal regime found over SWAC (biannual in observations) has been linked to an unrealistic seasonal cycle of SST and erroneous SST/rainfall relationships in this region. Additional work is merited to further elucidate exact mechanisms that determine the realistic representation of certain features and improve physical mechanisms represented by coupled simulations. Climate model projections should be treated with caution, and projections of future agriculture production in this region are likely to be unrealistic, due to the significant impact of the LDS on crop yields (Adejuwon and Odekunle 2006).

In conclusion, on a continental scale, the resemblance of spatial progression patterns thus adds credence to GCM future projections (Tierney *et al* 2015). However, in regions where the rainfall seasonal cycle is not well captured, caution should be exercised when interpreting climate change projections for impact assessment. The information in figures S24–26 on timing biases for individual models can be used to inform future studies on suitable model selection, reducing the inclusion of models with timing biases.

Acknowledgments, samples, and data

The authors would like to thank two anonymous reviewers for their insightful and constructive comments.

We acknowledge the World Climate Research Programme's Working Group on Coupled Modelling, which is responsible for CMIP, and we thank the climate modeling groups (models listed in table S1) for producing and making available their model outputs; for CMIP, the US Department of Energy's PCMDI provided coordinating support and led development of software infrastructure in partnership with the Global Organization for Earth System Science Portals. Model data were sourced from the CMIP5 data portal (http://cmip-pcmdi.llnl.gov/cmip5/data_portal.html) and the British Atmospheric Data Centre (http://badc.nerc.ac.uk/).

All observational datasets exploited are publicly available datasets. ARCv2 data can be obtained from ftp://ftp.cpc.ncep.noaa.gov/fews/fewsdata/africa/arc2/bin/. The TARCATv2 dataset is available from the TAMSAT website (www.met.reading.ac.uk/~tamsat/data). The CHIRPS dataset, produced by the Climate Hazards Group, is available at http://chg.geog.ucsb.edu/data/chirps/#_Data. GPCP daily data are available from http://precip.gsfc.nasa.gov/. The TRMM 3B42 data were obtained from http://pmm.nasa.gov/data-access/downloads/trmm.

Monthly HadISST observed SST was obtained from the UK Met Office: www.metoffice.gov.uk/hadobs/hadisst/data/download.html and monthly AMIP forcing SST data was obtained from www-pcmdi.llnl.gov/projects/amip/AMIP2EXPDSN/BCS/amipbc_dwnld.php.

Caroline M Dunning was supported with funding from a Natural Environment Research Council (NERC) PhD Studentship through the SCENARIO Doctoral Training Partnership grant NE/L002566/1. Richard P Allan's contribution to the research leading to these results has received funding from the National Centre for Earth Observation and the European Union 7th Framework Programme (FP7/2007–2013) under grant agreement 603502 (EU project DACCIWA: Dynamics-aerosol-chemistry-cloud interactions in West Africa). Emily Black's contribution to the research has been supported by the National

Centre for Atmospheric Science (Climate division), the NERC/DFID BRAVE project (NE/M008983/1) the NERC/DFID HyCristal project (NE/M020371/1) and the Global Challenges Research Fund ERADACS project (NE/P015352/1).

ORCID iDS

Caroline M Dunning https://orcid.org/0000-0002-7311-7846
Richard P Allan https://orcid.org/0000-0003-0264-9447

References

Adejuwon J O and Odekunle T O 2006 Variability and the severity of the 'Little Dry Season' in southwestern Nigeria *J. Clim.* **19** 483–93

Adhikari U, Nejadhashemi A P and Woznicki S A 2015 Climate change and Eastern Africa: a review of impact on major crops *Food Energy Secur.* **4** 110–32

Camberlin P, Moron V, Okoola R, Philippon N and Gitau W 2009 Components of rainy seasons variability in equatorial East Africa: onset, cessation, rainfall frequency and intensity *Theor. Appl. Climatol.* **98** 237–49

Caminade C, Kovats S, Rocklov J, Tompkins A M, Morse A P, Colón-González F J and Lloyd S J 2014 Impact of climate change on global malaria distribution *Proc. Natl Acad. Sci.* **111** 3286–91

Chang P, Zhang R, Hazeleger W, Wen C, Wan X, Ji L and Seidel H 2008 Oceanic link between abrupt changes in the North Atlantic ocean and the African monsoon *Nat. Geosci.* **1** 444–8

Chineke T C, Jagtap S S and Nwofor O 2010 West African monsoon: is the August break 'breaking' in the eastern humid zone of Southern Nigeria? *Clim. Change* **103** 555–70

Christensen J H *et al* 2013 Climate phenomena and their relevance for future regional climate change *Climate Change 2013: the Physical Science Basis Contribution of Working Group I to the Fifth Assessment Report of the Intergovernmental Panel on Climate Change* ed T F Stocker, D Qin, G K Plattner, M Tignor, S K Allen, J Boschung, A Nauels, Y Xia and V Bex and Midgley P M (Cambridge: Cambridge University Press) pp 1217–1308

Cook K H and Vizy E K 2006 Coupled model simulations of the West African monsoon system: twentieth- and twenty-first-century simulations *J. Clim.* **19** 3681–703

Dedekind Z, Engelbrecht F A and Van der Merwe J 2016 Model simulations of rainfall over Southern Africa and its eastern escarpment *Water SA* **42** 129–43

De Wit M and Stankiewicz J 2006 Changes in surface water supply across Africa with predicted climate change *Science* **311** 1917–21

Diem J E, Ryan S J, Hartter J and Palace M W 2014 Satellite-based rainfall data reveal a recent drying trend in central equatorial Africa *Clim. Change* **126** 263–72

Dike V N, Shimizu M H, Diallo M, Lin Z, Nwofor O K and Chineke T C 2015 Modelling present and future African climate using CMIP5 scenarios in HadGEM2-ES *Int. J. Climatol.* **35** 1784–99

Dunning C M, Black E C L and Allan R P 2016 The onset and cessation of seasonal rainfall over Africa *J. Geophys. Res. Atmos.* **121** 405–24

Endris H S *et al* 2013 Assessment of the performance of CORDEX regional climate models in simulating East African rainfall *J. Clim.* **26** 8453–75

Engelbrecht C J, Landman W A, Engelbrecht F A and Malherbe J 2015 A synoptic decomposition of rainfall over the cape south coast of South Africa *Clim. Dyn.* **44** 2589–607

Flato G *et al* 2013 Evaluation of climate models *Climate Change 2013: the Physical Science Basis Contribution of Working Group I to the Fifth Assessment Report of the Intergovernmental Panel on Climate Change, Climate Change* (Cambridge: Cambridge University Press) pp 741–866

Funk C *et al* 2015 The climate hazards infrared precipitation with stations-a new environmental record for monitoring extremes *Sci. Data* **2** 150066

GRUMP: Global Urban-Rural Mapping Project 2000 Population Density: Africa Socioeconomic Data and Applications Center (SEDAC) (http://sedac.ciesin.columbia.edu/data/collection/grump-v1/maps/gallery/search)

Hagos S M and Cook K H 2009 Development of a coupled regional model and its application to the study of interactions between the West African monsoon and the eastern tropical Atlantic ocean *J. Clim.* **22** 2591–604

Hamududu B and Killingtveit A 2012 Assessing climate change impacts on global hydropower *Energies* **5** 305–22

Herrmann S M and Mohr K I 2011 A continental-scale classification of rainfall seasonality regimes in Africa based on gridded precipitation and land surface temperature products *J. Appl. Meteorol. Climatol.* **50** 2504–13

Hill P G, Allan R P, Chiu J C and Stein T H M 2016 A multisatellite climatology of clouds, radiation, and precipitation in southern West Africa and comparison to climate models *J. Geophys. Res. Atmos.* **121** 857–10 879

Huffman G J, Adler R F, Morrissey M M, Bolvin D T, Curtis S, Joyce R, McGavock B and Susskind J 2001 Global precipitation at one-degree daily resolution from multisatellite observations *J. Hydrometeorol.* **2** 36–50

Huffman G J, Bolvin D T, Nelkin E J, Wolff D B, Adler R F, Gu G, Hong Y, Bowman K P and Stocker E F 2007 The TRMM multisatellite precipitation analysis (TMPA): quasi-global, multiyear, combined-sensor precipitation estimates at fine scales *J. Hydrometeorol.* **8** 38–55

Issa Lélé M and Lamb P J 2010 Variability of the intertropical front (ITF) and rainfall over the West African Sudan-Sahel zone *J. Clim.* **23** 3984–4004

Koutroulis A G, Grillakis M G, Tsanis I K and Papadimitriou L 2016 Evaluation of precipitation and temperature simulation performance of the CMIP3 and CMIP5 historical experiments *Clim. Dyn.* **47** 1881–98

Kumar D, Kodra E and Ganguly A R 2014 Regional and seasonal intercomparison of CMIP3 and CMIP5 climate model ensembles for temperature and precipitation *Clim. Dyn.* **43** 2491–518

Laloë J O, Cozens J, Renom B, Taxonera A and Hays G C 2014 Effects of rising temperature on the viability of an important sea turtle rookery *Nat. Clim. Change* **4** 513–8

Lee J-Y and Wang B 2014 Future change of global monsoon in the CMIP5 *Clim. Dyn.* **42** 101–19

Lyon B and DeWitt D G 2012 A recent and abrupt decline in the East African long rains *Geophys. Res. Lett.* **39** L02702

Liebmann B, Bladé I, Kiladis G N, Carvalho L M V, Senay G B, Allured D, Leroux S and Funk C 2012 Seasonality of African precipitation from 1996 to 2009 *J. Clim.* **25** 4304–22

Liu P, Meehl G A and Wu G 2002 Multi-model trends in the Sahara induced by increasing CO_2 *Geophys. Res. Lett.* **29** 1881

Maidment R I, Allan R P and Black E 2015 Recent observed and simulated changes in precipitation over Africa *Geophys. Res. Lett.* **42** 8155–64

Maidment R I, Grimes D, Allan R P, Tarnavsky E, Stringer M, Hewison T, Roebeling R and Black E 2014 The 30 year TAMSAT African rainfall climatology and time series (TARCAT) data set *J. Geophys. Res. Atmos.* **119** 10619–44

Maidment R I, Grimes D, Black E, Tarnavsky E, Young M, Greatrex H and Alcántara E M U 2017 A new, long-term daily satellite-based rainfall dataset for operational monitoring in Africa *Sci. Data* **4** 170063

Marteau R, Moron V and Philippon N 2009 Spatial coherence of monsoon onset over western and central Sahel (1950–2000) *J. Clim.* **22** 1313–24

McHugh M J 2005 Multi-model trends in East African rainfall associated with increased CO_2 *Geophys. Res. Lett.* **32** L01707

McSweeney C, Lizcano G, New M and Lu X 2010 The UNDP climate change country profiles: improving the accessibility of observed and projected climate information for studies of climate change in developing countries *Bull. Am. Meteorol. Soc.* **91** 157–66

Mehran A, AghaKouchak A and Phillips T J 2014 Evaluation of CMIP5 continental precipitation simulations relative to satellite-based gauge-adjusted observations *J. Geophys. Res. Atmos.* **119** 1695–707

Monerie P A, Sanchez-Gomez E and Boé J 2017 On the range of future Sahel precipitation projections and the selection of a sub-sample of CMIP5 models for impact studies *Clim. Dyn.* **48** 2751–70

Mounkaila M S, Abiodun B J and Omotosho J B 2015 Assessing the capability of CORDEX models in simulating onset of rainfall in West Africa *Theor. Appl. Climatol.* **119** 255–72

Nnamchi H C, Li J, Kucharski F, Kang I S, Keenlyside N S, Chang P and Farneti R 2015 Thermodynamic controls of the Atlantic Niño *Nat. Commun.* **6** 8895

Novella N S and Thiaw W M 2013 African rainfall climatology version 2 for famine early warning systems *J. Appl. Meteorol. Climatol.* **52** 588–606

Odekunle T O 2010 An assessment of the influence of the inter-tropical discontinuity on inter-annual rainfall characteristics in Nigeria *Geogr. Res.* **48** 314–26

Odekunle T O and Eludoyin A O 2008 Sea surface temperature patterns in the gulf of Guinea: their implications for the spatio-temporal variability of precipitation in West Africa *Int. J. Climatol.* **28** 1507–17

Odekunle T O 2007 Predicting the variability and the severity of the 'Little Dry Season' in Southwestern Nigeria *Ife J. Sci.* **9** 93–108

Okumura Y and Xie S P 2004 Interaction of the Atlantic equatorial cold tongue and the African monsoon *J. Clim.* **17** 3589–602

Olaniran O J 1989 The July–August rainfall anomaly in Nigeria *Climatol. Bull.* **22** 26–38

Patricola C M, Li M, Xu Z, Chang P, Saravanan R and Hsieh J S 2012 An investigation of tropical Atlantic bias in a high-resolution coupled regional climate model *Clim. Dyn.* **39** 2443–63

Reason C J C, Landman W and Tennant W 2006 Seasonal to decadal prediction of Southern African climate and its links with variability of the Atlantic Ocean *Bull. Am. Meteorol. Soc.* **87** 941–55

Richter I and Xie S P 2008 On the origin of equatorial Atlantic biases in coupled general circulation models *Clim. Dyn.* **31** 587–98

Roehrig R, Bouniol D, Guichard F, Hourdin F and Redelsperger J L 2013 The present and future of the West African monsoon: a process-oriented assessment of CMIP5 simulations along the AMMA transect *J. Clim.* **26** 6471–505

Shongwe M E, Van Oldenborgh G J, Van Den Hurk B J J M, De Boer B, Coelho C A S and Van Aalst M K 2009 Projected changes in mean and extreme precipitation in Africa under global warming. Part I: Southern Africa *J. Clim.* **22** 3819–37

Shongwe M E, Lennard C, Liebmann B, Kalognomou E-A, Ntsangwane L and Pinto I 2015 An evaluation of CORDEX regional climate models in simulating precipitation over Southern Africa *Atmos. Sci. Lett.* **16** 199–207

Siongco A C, Hohenegger C and Stevens B 2015 The Atlantic ITCZ bias in CMIP5 models *Clim. Dyn.* **45** 1169

Sultan B and Janicot S 2003 The West African monsoon dynamics. Part II: the preonset and onset of the summer monsoon, *J. Clim.* **16** 3407–27

Tanser F C, Sharp B and Le Sueur D 2003 Potential effect of climate change on malaria transmission in Africa *Lancet* **362** 1792–8

Tarnavsky E, Grimes D, Maidment R, Black E, Allan R P, Stringer M, Chadwick R and Kayitakire F 2014 Extension of the TAMSAT satellite-based rainfall monitoring over Africa and from 1983 to present *J. Appl. Meteorol. Climatol.* **53** 2805–22

Taylor K, Stouffer R and Meehl G 2012 An overview of CMIP5 and the experiment design *Bull. Amer. Meteor. Soc.* **93** 485–98

Tierney J E and Ummenhofer C C and deMenoca P B 2015 Past and future rainfall in the Horn of Africa *Sci. Adv.* **1** e1500682

Toniazzo T and Woolnough S 2014 Development of warm SST errors in the southern tropical Atlantic in CMIP5 decadal hindcasts *Clim. Dyn.* **43** 2889

van Vilet M T, Wiberg D, Leduc S and Riahi K 2016 Power-generation system vulnerability and adaptation to changes in climate and water resources *Nat. Clim. Change* **6** 375–80

Vizy E K and Cook K H 2001 Mechanisms by which Gulf of Guinea and eastern North Atlantic sea surface temperature anomalies can influence African rainfall *J. Clim.* **14** 795–821

Vizy E K, Cook K H, Chimphamba J and McCusker B 2015 Projected changes in Malawi's growing season *Clim. Dyn.* **45** 1673–98

Weldon D and Reason C J C 2014 Variability of rainfall characteristics over the south coast region of South Africa *Theor. Appl. Climatol.* **115** 177–85

Yamada T J, Kanae S, Oki T and Koster R D 2013 Seasonal variation of land-atmosphere coupling strength over the West African monsoon region in an atmospheric general circulation model *Hydrol. Sci. J.* **58** 1276–86

Yamana T K, Bomblies A and Eltahir E A 2016 Climate change unlikely to increase malaria burden in West Africa *Nat. Clim. Change* **6** 1009–13

Yamba F D, Walimwipi H, Jain S, Zhou P, Cuamba B and Mzezewa C 2011 Climate change/variability implications on hydroelectricity generation in the Zambezi river basin *Mitig. Adapt. Strat. Glob. Change* **16** 617–28

Yang W, Seager R, Cane M A and Lyon B 2015a The rainfall annual cycle bias over East Africa in CMIP5 coupled climate models *J. Clim.* **28** 9789–802

Yang W, Seager R, Cane M A and Lyon B 2015b The annual cycle of East African precipitation *J. Clim.* **28** 2385–404